

See discussions, stats, and author profiles for this publication at: <https://www.researchgate.net/publication/51244039>

Discovery of Naturally Occurring Aurones That Are Potent Allosteric Inhibitors of Hepatitis C Virus RNA-Dependent RNA Polymerase

ARTICLE *in* JOURNAL OF MEDICINAL CHEMISTRY · JUNE 2011

Impact Factor: 5.45 · DOI: 10.1021/jm200242p · Source: PubMed

CITATIONS

36

READS

123

10 AUTHORS, INCLUDING:



Romain Haudecoeur

University Joseph Fourier - Grenoble 1

21 PUBLICATIONS 166 CITATIONS

SEE PROFILE



Abdelhakim Ahmed-Belkacem

French Institute of Health and Medical Resea...

18 PUBLICATIONS 582 CITATIONS

SEE PROFILE



Edwige Nicolle

University Joseph Fourier - Grenoble 1

11 PUBLICATIONS 287 CITATIONS

SEE PROFILE



AHCène Boumendjel

University Joseph Fourier - Grenoble 1

130 PUBLICATIONS 2,193 CITATIONS

SEE PROFILE

Discovery of Naturally Occurring Aurones That Are Potent Allosteric Inhibitors of Hepatitis C Virus RNA-Dependent RNA Polymerase

Romain Haudecoeur,^{†,‡} Abdelhakim Ahmed-Belkacem,^{‡,§} Wei Yi,[†] Antoine Fortuné,[†] Rozenn Brillet,[‡] Catherine Belle,[§] Edwige Nicolle,[†] Coralie Pallier,^{‡,||} Jean-Michel Pawlowsky,^{‡,⊥,∞} and AHCène Boumendjel^{*,†,∞}

[†]Département de Pharmacochimie Moléculaire, Université de Grenoble, CNRS, UMR 5063, BP 53, 38041 Grenoble Cedex 9, France

[‡]Hôpital Henri Mondor, INSERM U955, 51 Avenue du Maréchal de Lattre de Tassigny, 94010 Créteil, France

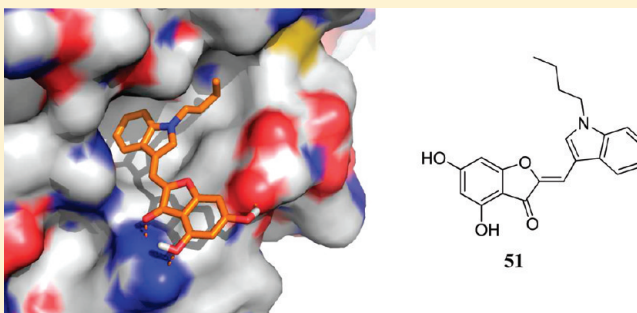
[§]Département de Chimie Moléculaire, Université de Grenoble, CNRS, UMR 5250, BP 53, 38041 Grenoble Cedex 9, France

^{||}Department of Virology, Hôpital de Bicêtre, Le Kremlin-Bicêtre, France

[⊥]Department of Virology, Hôpital Henri Mondor, National Reference Center for Viral Hepatitis B, C and Delta, Université Paris-Est, 51 Avenue du Maréchal de Lattre de Tassigny, 94010 Créteil, France

S Supporting Information

ABSTRACT: We have identified naturally occurring 2-benzylidenebenzofuran-3-ones (aurones) as new templates for non-nucleoside hepatitis C virus (HCV) RNA-dependent RNA polymerase (RdRp) inhibitors. The aurone target site, identified by site-directed mutagenesis, is located in thumb pocket I of HCV RdRp. The RdRp inhibitory activity of 42 aurones was rationally explored in an enzyme assay. Molecular docking studies were used to determine how aurones bind to HCV RdRp and to predict their range of inhibitory activity. Seven aurone derivatives were found to have potent inhibitory effects on HCV RdRp, with IC₅₀ below 5 μ M and excellent selectivity index (inhibition activity versus cellular cytotoxicity). The most active aurone analogue was (Z)-2-((1-butyl-1H-indol-3-yl)methylene)-4,6-dihydroxybenzofuran-3(2H)-one (compound **51**), with an IC₅₀ of 2.2 μ M. Their potent RdRp inhibitory activity and their low toxicity make these molecules attractive candidates as direct-acting anti-HCV agents.



INTRODUCTION

Hepatitis C virus (HCV) infection is a global public health problem. The World Health Organization (WHO) estimates that 120–140 million people are infected worldwide (2–3% of the world population), while 3–4 million are newly infected each year. Chronic HCV infection is associated with chronic liver inflammation and fibrosis. In the absence of antiviral treatment, HCV liver disease progresses to cirrhosis in 20–30% of chronically infected patients, and patients with cirrhosis have a 1–4% annual risk of developing hepatocellular carcinoma.¹ HCV infection is curable. The current standard of care is a combination of pegylated interferon α (peg-IFN) and ribavirin (RBV).^{2–5} Unfortunately, the response rate is low, especially among patients infected by HCV genotype 1, the most frequent genotype in the U.S., Europe, Asia, and Latin America (60–75% of cases).⁶ In 2012, a new treatment based on a combination of peg-IFN, ribavirin, and a direct-acting antiviral drug that inhibits HCV serine protease activity (telaprevir or boceprevir) will be available for patients with HCV genotype 1 infection. Yet these new therapies will fail in 20–30% of treatment-naïve patients and in about 50% of patients in whom a first course of peg-IFN and

ribavirin has failed to eradicate the infection. Thus, as a preventive vaccine will not be available for several years, there is an urgent need for more effective anti-HCV drugs.

The HCV RNA-dependent RNA polymerase (RdRp) is a particularly attractive target because of its key role in viral replication and the fact that this enzyme has no functional equivalent in mammalian cells. A number of HCV RdRp inhibitors have been identified, including nucleoside/nucleotide analogues that target the active site, and non-nucleoside allosteric inhibitors.^{7,8} The HCV RdRp structure resembles a right hand. Four allosteric binding sites have been identified so far, including “thumb” pockets I and II and “palm” pockets I and II.^{8,9} To date, two classes of molecules sharing a number of similarities have been reported to bind to thumb pocket I, including 2-aryl-1-cyclohexylbenzimidazole-5-carboxylic acid derivatives and their indole-based equivalents (Figure 1).^{10–17} Some of these compounds are currently being tested in HCV-infected patients. For example, a phase I clinical trial of MK-3281, an indole-based thumb pocket I inhibitor,¹⁷ has recently been completed.¹⁸

Received: March 1, 2011

Published: June 23, 2011

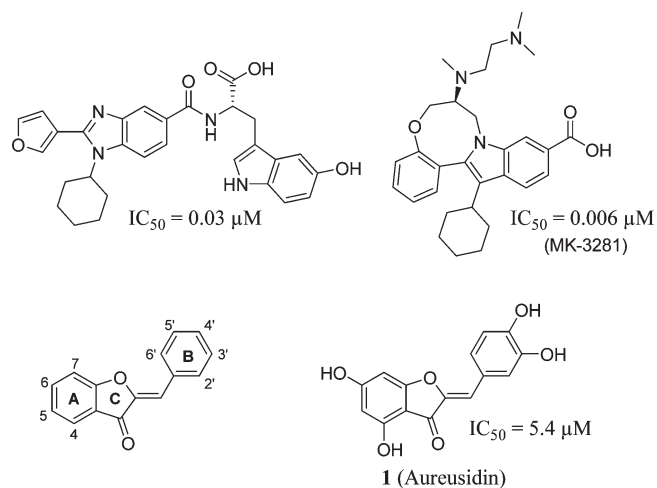
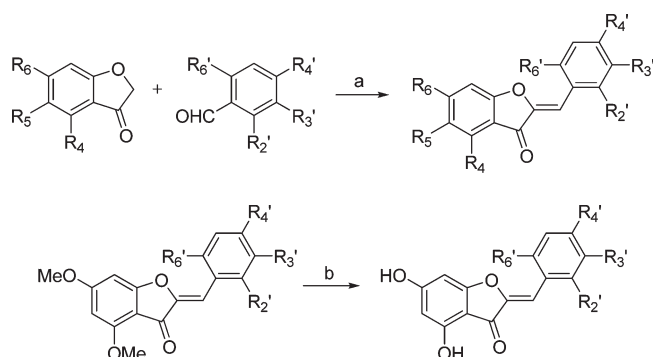


Figure 1. Two examples of known thumb pocket I inhibitors (top),^{16,17} general structure of the aureone backbone (bottom left), and structure of naturally occurring aureusidin (compound 1, bottom right).

Scheme 1. Synthesis of Aurone Derivatives, Starting from Building Blocks 2–9^a



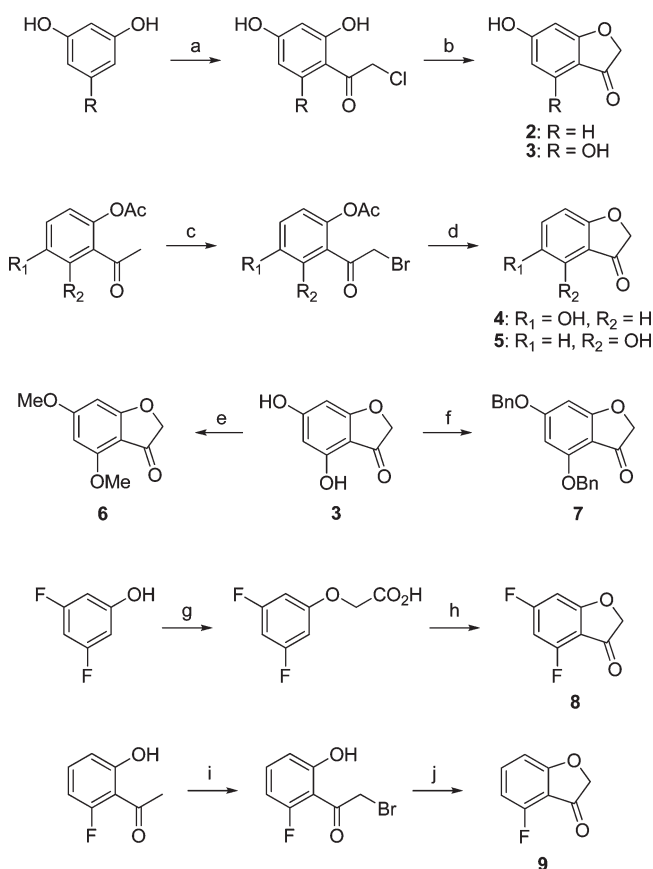
^a Reagents and conditions. (a) For procedure A: KOH/MeOH, 60 °C, 1–18 h. For procedure B: KOH/EtOH, 80 °C, 2–5 h. For procedure C: Al_2O_3 , CH_2Cl_2 , room temp, 16 h. (b) BBr_3 , CH_2Cl_2 , 0 °C to room temp, 24–72 h.

Aurones (2-benzylidenebenzofuran-3-ones) are naturally occurring small molecules belonging to the flavonoid family, the pharmacological potential of which we reported for the first time several years ago.¹⁹ As part of an ongoing program investigating the therapeutic potential of aurones, we discovered that aureusidin (3',4,4',6-tetrahydroxyaurone, 1, Figure 1),^{20,21} a naturally occurring aurone, potently inhibits HCV RdRp with an IC_{50} of 5.2 μM . Interestingly, the cellular toxicity of aurone 1 against mammalian cells occurs at very higher concentration (>400 μM). Mutagenic studies and molecular modeling identified thumb pocket I as the aurone binding site. On the basis of these preliminary data, we used the aureone scaffold as a template for the design of aureone analogues with potent inhibitory activity on HCV RdRp.

CHEMISTRY

The aureone derivatives described in this study were synthesized by means of aldol condensation of a substituted benzofuran-3(2H)-one with a benzaldehyde derivative, in basic KOH/MeOH conditions under reflux. Aurones bearing fluoro groups were

Scheme 2. Synthesis of Benzofuran-3(2H)-one Derivatives 2–9 as the Key Starting Blocks^a

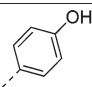
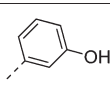
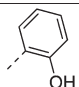
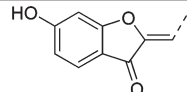
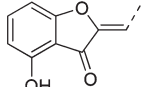
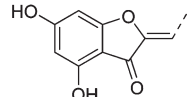
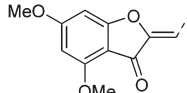


^a Reagents and conditions: (a) $ClCH_2CN$, HCl, $ZnCl_2$, Et_2O , then HCl, H_2O , 100 °C, 1 h; (b) MeONa, MeOH, 60 °C, 1.5 h; (c) trimethylphenylammonium tribromide, THF, room temp, 6 h; (d) KOH, MeOH, 60 °C, 3 h; (e) Me_2SO_4 , K_2CO_3 , dimethoxyethane, 80 °C, 3 h; (f) BnBr, K_2CO_3 , dimethoxyethane, room temp, 3 days; (g) chloroacetic acid, NaOH, H_2O , 90 °C, 18 h; (h) $SOCl_2$, PhMe, 110 °C, 2 h, then $AlCl_3$, CH_2Cl_2 , 40 °C, 18 h; (i) $CuBr_2$, EtOAc, $CHCl_3$, 60 °C, 18 h; (j) K_2CO_3 , DMF, 0 °C, 1.5 h.

obtained with a softer method using neutral alumina, as described by Varma et al., in order to avoid nucleophilic substitutions by in situ formed potassium methoxide.²² 4,6-Dihydroxyaurones were synthesized by preparing the corresponding 4,6-dimethoxy analogues, followed by deprotection with boron tribromide. In some cases it was possible to obtain these derivatives directly by simple basic condensation in KOH/EtOH (Scheme 1).

These pathways required the synthesis of benzofuran-3(2H)-ones 2–9 by various methods, as described elsewhere (Scheme 2). Compounds 2 and 3 were synthesized from resorcinol and phloroglucinol, respectively. By use of chloroacetonitrile in HCl/ Et_2O , electrophilic addition in the ortho position from one of the hydroxyl groups allowed the recovery of the chloroacetophenone. Cyclization then readily occurred in NaOMe/MeOH.²³ Further reaction of 3 with methyl sulfate (Me_2SO_4) or benzyl bromide (BnBr) in the presence of K_2CO_3 yielded 6 or 7, respectively.²⁴ Compounds 4 and 5 were obtained from the corresponding diacetoxyacetophenones after bromination of the α -position of the ketone with triphenylmethylammonium tribromide and then one-pot deprotection and cyclization

Table 1. Initial Array of NSSB Inhibition by Aureusidin Analogues (Compounds 10–20)

									
	Cd	Inh. (20 μ M, %)	IC ₅₀ (μ M)	Cd	Inh. (20 μ M, %)	IC ₅₀ (μ M)	Cd	Inh. (20 μ M, %)	IC ₅₀ (μ M)
	10	35±3	n.d.	14	10±0.7	n.d.	17	18±3	n.d.
	11	60±4	5.9±0.3	15	37±1	n.d.	18	56±1	11.1±0.4
	12	61±2	9.7±0.1				19	33±2	n.d.
	13	37±3	n.d.	16	11±2	n.d.	20	0.7±1	n.d.

in KOH/MeOH.²⁵ The same approach was used for compound **9** but with direct bromination of the 2-fluoro-6-hydroxyacetophenone with CuBr₂, then cyclization in a K₂CO₃/DMF medium. Compound **8** was obtained from 3,5-difluorophenol, which was alkylated with chloroacetic acid. Subsequent chlorination of the acid, followed by Friedel–Crafts cyclization, yielded the desired compound.²⁷

Benzaldehyde derivatives were purchased from commercial sources or synthesized using published approaches. 4-Cyclohexylbenzaldehyde was synthesized from cyclohexylbenzene in a formylation reaction, using hexamethylenetetramine in TFA.²⁷ 1-Butyl-1*H*-indole-3-carbaldehyde was obtained from indole-3-carbaldehyde and butyl bromide, using NaH in DMF.

RESULTS AND DISCUSSION

An enzyme assay was used to assess the inhibition of the polymerase activity of a purified RdRp (nonstructural SB [NSSB] protein), deleted of its 21 C-terminal amino acids in order to ensure solubility (HCV-NSSBΔ21). The J4 genotype 1b reference strain was used. This assay measures the amount of double-stranded RNA synthesized in the presence of HCV-NSSBΔ21, a homopolymeric RNA template and ATP, as previously described.²⁸ Initial screening was performed at an aurone concentration of 20 μ M. The naturally occurring aureusidin (**1**, Figure 1) was found to be a potent inhibitor of HCV-NSSBΔ21 enzyme activity (85% inhibition at 20 μ M, IC₅₀ = 5.4 \pm 1.9 μ M). This compound served as a “hit” for our subsequent investigations. As most naturally occurring aurones are hydroxylated at positions 4, 6, 2', 3', and 4' (see Figure 1), we first investigated aurones bearing two or three hydroxy groups at the above-mentioned positions (Table 1). At the A-ring, the presence of a hydroxyl group at position 4 seemed to be crucial, as 4-hydroxy and 4,6-dihydroxy derivatives **11** and **12** showed a one-digit micromolar range IC₅₀ (respectively 5.9 and 9.7 μ M) and as deletion of this 4-hydroxy group provided an inactive compound (IC₅₀ > 20 μ M for **10**). Replacement of the hydroxy substituents at positions 4 and 6 by methoxy groups also resulted in an important drop of activity (IC₅₀ > 20 μ M for **13**). At the

B-ring, considering the 4-hydroxy derivatives, position 4' appeared to be the most beneficial for activity (IC₅₀ = 5.9 μ M for **11**), since the 2'-hydroxylated analogue led to a 2-fold loss of activity (IC₅₀ = 11.1 μ M for **18**) and the 3'-hydroxylated derivative was almost inactive (IC₅₀ > 20 μ M for **15**). These preliminary results designed a substitution pattern in which the positions 4, 6, and 4' constituted the most promising ones for further explorations.

In order to check the antiviral potential of aurones, we evaluated the inhibition effect of aurones **11** and **12** on the HCV replication in JFH1 (HCV) cell based assays. Aurones **11** and **12** showed IC₅₀ of 18 \pm 7 and 40 \pm 4 μ M, respectively.

The next step was to identify the aurone binding site in HCV RdRp. Four sites, thumb pockets I and II and palm pockets I and II, have been identified through X-ray structure of crystallized complexes as binding sites for non-nucleoside allosteric inhibitors of HCV RdRp (Figure 2). Amino acid substitutions at these sites have been shown to reduce susceptibility to the corresponding inhibitors. In order to determine if aurones target one of these sites, we examined whether these substitutions reduced HCV RdRp susceptibility to aurones in our cell-free enzyme assay. For this purpose we engineered HCV-NSSBΔ21 carrying the P495L, M423T, C316Y, or H95Q substitutions that are known to confer resistance to reported inhibitors.²⁹ The experiments were carried out with (Z)-2-(4-hydroxybenzylidene)-4-hydroxybenzofuran-3(2*H*)-one (**11**). The IC₅₀ values of **11** for each HCV-NSSBΔ21 mutant were compared with the IC₅₀ for wild-type HCV-NSSBΔ21, and the results were recorded as fold differences (Figure 3). A benzimidazole, 2-[4-[(4-(acetylamino)-4'-chloro-[1,1'-biphenyl]-2-yl)methoxy]phenyl]-1-cyclohexyl-1*H*-benzimidazole-5-carboxylic acid, an inhibitor of HCV RdRp known to target thumb pocket I, was used as a control.³⁰ As expected, this latter compound was 10-fold less potent against HCV-NSSBΔ21-P495L than against HCV-NSSBΔ21-Wt, whereas its activity was not affected by the other amino acid substitutions. The inhibitory activity of aurone **11** was therefore only affected by the P495L substitution (as a 6- to 7-fold loss of activity), indirectly suggesting that this compound binds to (or close to) thumb pocket I. However, the lack of X-ray structure of an

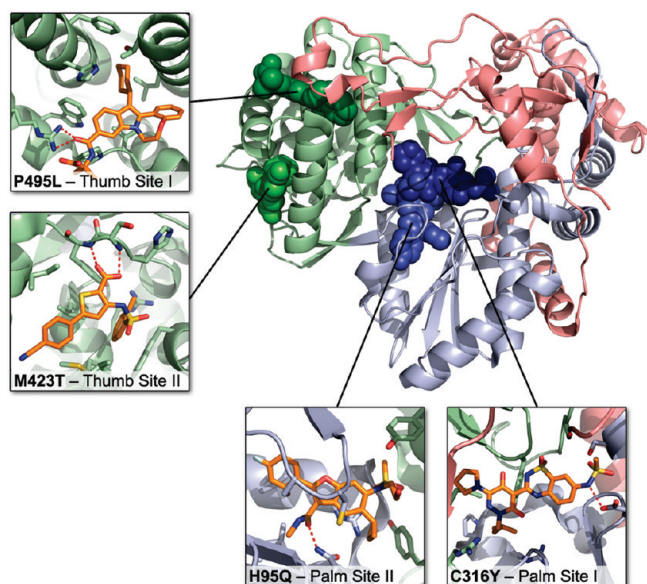


Figure 2. Structure of HCV RdRp with its three subdomains (fingers in red, palm in blue, and thumb in green) and its four allosteric binding sites for known non-nucleoside inhibitors. Key substitution sites of adjacent amino acids are indicated in bold.

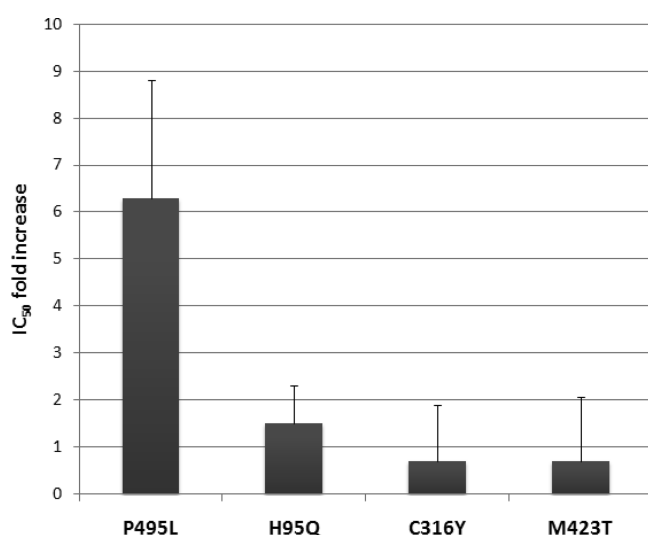


Figure 3. Fold increase in IC₅₀ relative to wild-type NS5BΔ21 obtained with aurone **11** and P495L, H95Q, C316Y, and M423T mutants. These mutations are known to reduce susceptibility to thumb pocket I, palm pocket II, palm pocket I, and thumb pocket II inhibitors, respectively.

aurone–NS5B complex, which would be a solid proof for the binding site of aurones, suggests caution in the interpretation of these results.

With the findings reported in Table 1 and the mutagenesis experiments in hand, we explored further the structure–activity relationship of NS5B inhibition by aurones (Table 2). At the B-ring, complete deletion of hydroxyl groups was followed by a 1.5- to 2.5-fold loss of activity (IC₅₀ of 14.6 μ M for **21** versus 5.9 μ M for **11**; IC₅₀ of 15.1 μ M for **33** versus 9.7 μ M for **12**). In contrast, the introduction of additional hydroxy groups at the B-ring led to 1.5- to 2.5-fold more active compounds (IC₅₀ of 5.4 μ M for the already described **1** and 5.8 μ M for **34** versus

9.7 μ M for **12**; IC₅₀ of 2.6 μ M for **22** versus 5.9 μ M for **11**), suggesting that 2',4'-dihydroxy and 3',4'-dihydroxy substitutions were favorable. The position 5 was also investigated, but the 4'-hydroxy derivative **49** did not exhibit significant activity.

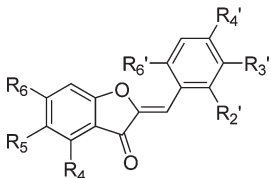
On the basis of the reported X-ray crystallographic structure of genotype 1b HCV RdRp complexed with a tetracyclic indole-based inhibitor binding to thumb pocket I (PDB code 2dxs),³⁰ docking calculations were used to rationalize the observed activities. The best poses generated with Autodock software for compound **1** showed that arginine 503 anchored the molecule, forming two hydrogen bonds with the 4-hydroxyl group and the ketone of the aurone. Glycine 493 allowed the formation of a third weaker hydrogen bond with the 6-hydroxy group. These findings could potentially explain the slightly better activities of 4,6-dihydroxyaurones compared to 4-hydroxyaurones, except for **22** which showed a 2.3-fold better activity than the corresponding 4,6-dihydroxylated **34**. At the B-ring, the 3'- and 4'-hydroxyl groups of **1** allowed the formation of two additional chelating hydrogen bonds with the carbonyl group of leucine 392 inside the hydrophobic pocket, as shown in Figure 4A. These findings could explain the strong impact of hydroxy groups at these positions. However, as stated above, 3'-hydroxylated aurones were almost inactive, whereas 4'-hydroxylated ones often provided some of the best observed activities, indicating a stronger influence of the 4'-position, not explained by this binding model.

In order to study the significance of the hydrophilicity and hydrogen bond donor potential of hydroxy substituents in aurones, we synthesized several compounds in which hydroxy groups were replaced by isosteric hydrophobic fluorine atoms. Compounds bearing 4-fluoro or 4,6-difluoro substituents were found as totally inactive molecules (**47** and **48**, fluoro analogues of **39** and **22**). This highlighted the crucial importance of the A-ring hydroxy substitution pattern as a hydrophilic and hydrogen bond donor moiety and seemed to confirm the docking indications about the key anchor role of this part of the inhibitors. On the other hand, the introduction of a fluorine atom in position 4' of the aurones affected very slightly the biological activity of the compound (IC₅₀ of 11.2 μ M for **42** versus 9.7 μ M for **12**), suggesting the possibility of introducing hydrophobic substituents at this part of the molecule.

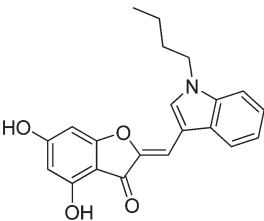
Given the strongly hydrophobic environment of thumb pocket I and the design of our structure–activity relationship, we considered testing the effect of hydrophobic substituents at the B-ring of aurones, especially at position 4'. Molecular docking based on the above known crystallographic structure (PDB code 2dxs) was used throughout the decision process as an indicator of the possibly relevant substituents and their positions. With the help of these tools, it appeared that the 4'-butyl and 4'-cyclohexyl moieties were wise choices. Indeed, the 4'-butyl and 4'-cyclohexyl aurones were the most active compounds of the 4,6-dihydroxy series (IC₅₀ of 2.3 and 2.5 μ M for **40** and **39**), but the 4'-ethyl or 4'-isopropyl groups provided derivatives in the same range of activity (IC₅₀ of 3.1 and 3.6 μ M for **38** and **37**). Interestingly, the 4-hydroxy analogues were 10-fold less active (IC₅₀ > 20 μ M for **27**, **28**, and **29**) except for the 2',4'-dimethyl derivative **23** (IC₅₀ = 5.8 μ M) and for the 4'-*N*-methylpiperazinyl derivative **31** (IC₅₀ = 3.8 μ M). Methoxy substituted derivatives did not reach inhibition values as well (IC₅₀ = 9.7 μ M for the best one **24**, and IC₅₀ > 20 μ M for **25**, **26**, and **36**).

Additionally, among a large number of virtual alternative structures, molecular modeling identified the replacement of the B-ring by substituted indole cores as potential candidates for

Table 2. Inhibition Activity of Compounds 1 and 21–51



1, 21 - 50



51

compd	R ₄	R ₅	R ₆	R _{2'}	R _{3'}	R _{4'}	R _{6'}	inhibition (20 μ M, %)	IC ₅₀ (μ M)
1	OH	H	OH	H	OH	OH	H	85 \pm 3	5.4 \pm 0.3
21	OH	H	H	H	H	H	H	57 \pm 3	14.6 \pm 0.6
22	OH	H	H	OH	H	OH	H	94 \pm 2	2.6 \pm 0.1
23	OH	H	H	Me	H	Me	H	64 \pm 1	5.8 \pm 0.2
24	OH	H	H	OMe	H	OMe	H	75 \pm 3	9.7 \pm 0.2
25	OH	H	H	OMe	H	H	OMe	47 \pm 2	nd
26	OH	H	H	OMe	H	OMe	OMe	52 \pm 1	nd
27	OH	H	H	H	H	Et	H	46 \pm 2	nd
28	OH	H	H	H	H	<i>i</i> -Pr	H	30 \pm 2	nd
29	OH	H	H	H	H	<i>n</i> -Bu	H	42 \pm 1	nd
30	OH	H	H	H	H	<i>t</i> -Bu	H	61 \pm 2	nd
31	OH	H	H	H	H	<i>N</i> -Me-Ppz	H	94 \pm 3	3.8
32	OH	H	H	F	H	H	H	58 \pm 5	nd
33	OH	H	OH	H	H	H	H	59 \pm 4	15.1 \pm 0.7
34	OH	H	OH	OH	H	OH	H	81 \pm 6	5.8 \pm 0.3
35	OH	H	OH	OMe	OMe	H	H	74 \pm 3	nd
36	OH	H	OH	OMe	OMe	OMe	H	50 \pm 2	nd
37	OH	H	OH	H	H	Et	H	79 \pm 7	3.6 \pm 0.2
38	OH	H	OH	H	H	<i>i</i> -Pr	H	78 \pm 4	3.1 \pm 0.1
39	OH	H	OH	H	H	<i>n</i> -Bu	H	93 \pm 4	2.5 \pm 0.1
40	OH	H	OH	H	H	<i>c</i> -Hex	H	92 \pm 2	2.3 \pm 0.2
41	OH	H	OH	H	H	morpholinyl	H	66 \pm 1	11.4 \pm 0.3
42	OH	H	OH	H	H	F	H	80 \pm 2	11.2 \pm 0.2
43	OMe	H	OMe	Me	H	Me	H	14 \pm 3	nd
44	OMe	H	OMe	H	H	<i>n</i> -Bu	H	3 \pm 2	nd
45	OMe	H	OMe	H	H	<i>c</i> -Hex	H	2 \pm 1	nd
46	H	H	H	H	H	<i>n</i> -Bu	H	−34 \pm 3	nd
47	F	H	F	H	H	<i>n</i> -Bu	H	−33 \pm 4	nd
48	F	H	H	F	H	F	H	10 \pm 2	nd
49	H	OH	H	H	H	OH	H	46 \pm 2	nd
50	OBn	H	OBn	H	H	<i>c</i> -Hex	H	3 \pm 3	nd
51								95 \pm 1	2.2 \pm 0.2

the improvement of the activity. In models built with GOLD and Autodock software, the best poses were obtained for *N*-alkylindole analogues ((*Z*)-2-(*N*-alkylindolyl)methylene)-4,6-dihydroxybenzofuran-3(2*H*)-one). Compound 51, which belongs to this group of indole derivatives, had a highly discriminant Goldscore of 52.4 (36.9–43.6 for compounds 23, 24, 27, 28, 29, 39, and 40). Arginine 503 was found to anchor the molecule in a similar way compared to compound 1, whereas hydrophobic residues (especially leucine 492, valine 37, alanine 393, leucine 392, alanine 396, alanine 395, phenylalanine 429, and isoleucine 424), forming two pockets, maintained both the indole part and the *N*-alkyl substituent of the ligand. The fixation mode of compound 51,

which had the strongest inhibitory activity (IC₅₀ = 2.2 μ M), is shown in Figure 4B. Although these findings were a useful indication of the binding mode and confirmed the inhibitory potential of this group of indole derivatives, the slight gain of biological activity (IC₅₀ of 2.2 μ M versus 2.5 μ M for 39 or 2.3 μ M for 40) did not reflect completely the good discrimination *in silico* between 51 and most of the other micromolar range inhibitors.

Overall, the docking results obtained with weak inhibitors were, as expected, difficult to interpret, but the geometries of poses obtained with more efficient compounds were often homogeneous and relevant. The strong activities of both B-hydroxylated and B-hydrophobic compounds could be explained

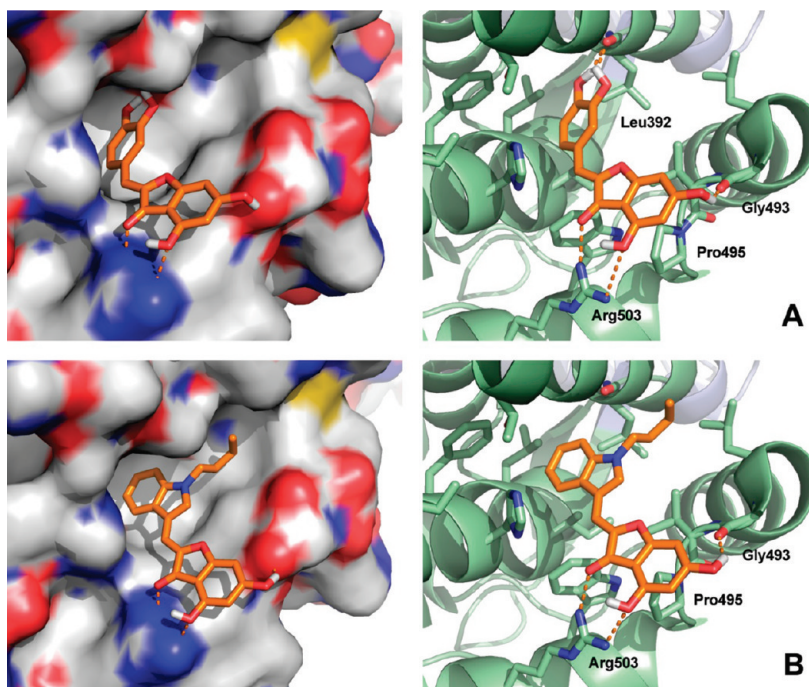


Figure 4. Surface and ribbon views of predicted binding modes in RdRp thumb pocket I of a reported X-ray structure (PDB code 2dxs) from docking studies with Autodock. (A) For compound **1**, involved in five hydrogen bonds: two with arginine 503 (1.9 Å and 2.5 Å), one with glycine 493 (1.8 Å), and two with leucine 392 (2.0 Å and 2.0 Å). (B) For compound **51**, involved in three hydrogen bonds: two with arginine 503 (1.8 Å and 2.0 Å) and one with glycine 493 (2.2 Å). The pictures were built with Pymol software.

by the good fit of these two subclasses of aurones in the pocket. Compounds **1** and **51** were representative of this hypothetical dual mode of aurone binding to thumb pocket I of HCV RdRp. Finally, in brief, we identified the following pharmacophoric elements as crucial in the inhibitory activity of aurones on HCV RdRp: (a) a hydroxy group at position 4 or a dihydroxy group at positions 4 and 6 and (b) a 2',4'- or 3',4'-dihydroxylated B-ring or a hydrophobic and bulky substituent or alternative core at the B-ring.

All the reported compounds were evaluated for cytotoxicity, based on the MTT assay with two human cell lines (HuH7 and HEK293). HuH7 and HEK293 cells were incubated in the presence of increasing concentrations of the tested compound, ranging from 0 to 512 μM . All reported compounds were not cytotoxic even at the highest concentration (data not shown).

CONCLUSION

We investigated the capacity of aurones, nontoxic natural compounds, to inhibit HCV RdRp. Aureusidin potently inhibited the activity of this enzyme. By using classical medicinal chemistry, we identified positions and substituents that are crucial for the inhibitory activity of aurones on RdRp. A combination of site-directed mutagenesis and molecular modeling was successfully used to understand and optimize aurones' anti-HCV activity. Our findings constitute a new starting point in the development of new non-nucleoside inhibitors of HCV RdRp. Studies are underway to synthesize more active compounds warranting preclinical evaluation.

EXPERIMENTAL SECTION

Chemistry. ^1H and ^{13}C NMR spectra were recorded on a Bruker AC-400 instrument (400 MHz for ^1H and 100 MHz for ^{13}C). Chemical

shifts (δ) are reported in ppm relative to Me_4Si (internal standard). Electrospray ionization ESI mass spectra were acquired by the Analytical Department of Grenoble University, France, on an Esquire 300 Plus Bruker Daltonis instrument with a nanospray inlet. Combustion analyses were performed at the Analytical Department of Grenoble University, and all tested compounds have a purity of at least 95%. Thin-layer chromatography (TLC) used Merck silica gel F-254 plates (thickness 0.25 mm). Flash chromatography used Merck silica gel 60, 200–400 mesh. All solvents were distilled prior to use. Unless otherwise stated, reagents were obtained from commercial sources and were used without further purification. Compounds **2**–**9** were prepared according to published procedures.^{23–27}

General Procedure A for the Preparation of (Z)-2-Benzylidenebenzofuran-3(2H)-one Derivatives. To a solution of a benzofuran-3(2H)-one derivative in methanol (15 mL/mmol) were added an aqueous solution of potassium hydroxide (50%, 1.5 mL/mmol) and a benzaldehyde derivative (1.5 equiv). The solution was then refluxed until TLC showed complete disappearance of the starting materials (1–18 h). After cooling, the mixture was concentrated under reduced pressure. Then the residue was diluted in water (50 mL/mmol), and an aqueous solution of hydrochloric acid (1 N) was added to adjust the pH to 2–3. The mixture was extracted with ethyl acetate or dichloromethane and washed with water and brine. The combined organic layers were dried over magnesium sulfate and filtered, and the filtrate was concentrated under reduced pressure to give the crude compound.

General Procedure B for the Preparation of (Z)-2-Benzylidenebenzofuran-3(2H)-one Derivatives. To a solution of a benzofuran-3(2H)-one derivative in ethanol (4 mL/mmol) were added an aqueous solution of potassium hydroxide (50%, 5 mL/mmol) and a benzaldehyde derivative (2 equiv). The solution was then refluxed until TLC showed complete disappearance of the starting materials (2–5 h). After cooling, the mixture was concentrated under reduced pressure. Then the residue was diluted in water (50 mL/mmol), and an aqueous

solution of hydrochloric acid (1 N) was added to adjust the pH to 2–3. The mixture was extracted with ethyl acetate or dichloromethane and washed with water and brine. The combined organic layers were dried over magnesium sulfate and filtered, and the filtrate was concentrated under reduced pressure to give the crude compound.

General Procedure C for the Preparation of (Z)-2-Benzylidenebenzofuran-3(2H)-one Derivatives. To a solution of a benzofuran-3(2H)-one derivative in anhydrous dichloromethane (20 mL/mmol) were added a benzaldehyde derivative (1.5 equiv) and aluminum oxide (4000 mg/mmol). The suspension was stirred under argon overnight, and the solid was removed by filtration. The filtrate was distilled under reduced pressure to give the crude compound.

General Procedure D for the Preparation of (Z)-2-Benzylidenebenzofuran-3(2H)-one Derivatives. To a solution of a (Z)-2-benzylidenebenzofuran-3(2H)-one derivative in anhydrous dichloromethane (10 mL/mmol) was added pure boron tribromide (20 equiv) at 0 °C. The solution was then stirred at room temperature until TLC showed complete disappearance of the starting materials (24–72 h). Cold water was then added, and the suspension was extracted three times with ethyl acetate and washed with water and brine. The combined organic layers were dried over magnesium sulfate and filtered, and the filtrate was concentrated under reduced pressure to give the crude compound.

Molecular Modeling. Docking studies used the reported X-ray crystallographic structure of HCV genotype 1b RdRp complexed with a known inhibitor binding to thumb pocket I of the enzyme (PDB code 2dxs).³¹ The protein structure was extracted, and water molecules were deleted. The complexed ligand was used to define the binding site for docking and was successfully docked in a similar conformation in the pocket, using the same protocol as for aurones. The genetic algorithms of GOLD and Autodock4 docking software performed flexible docking with small molecules while keeping the protein structure rigid. All compounds were built and their energies minimized with Sybyl, using a conjugate gradient method and MMFF94 force field and charges. For each compound, 20 poses were generated by GOLD and ranked according to the Goldscore scoring function, while 100 poses were generated by Autodock and clustered according to their spatial proximity and calculated free energy of binding. Molecular surfaces were generated with MOLCAD, and the docking solutions were analyzed with Sybyl.

Biology. Expression and Purification of Recombinant HCV NSSBΔ21. RdRp (NSSB protein) from the HCV J4 genotype 1b reference strain, truncated of its 21 C-terminal amino acids to ensure solubility (NSSBΔ21) and carrying a hexahistidine tag (His-Tag) at its N-terminus, was expressed in *Escherichia coli* C41(DE3) and purified. Chromatography was performed on Ni-NTA columns (Qiagen, Valencia, CA). The columns were washed with a buffer containing 50 mM NaH₂PO₄ (pH 8.0), 500 mM NaCl, and 20 mM imidazole. The bound protein was eluted in 1 mL fractions with a buffer containing 50 mM NaH₂PO₄ (pH 8.0), 500 mM NaCl, and 250 mM imidazole. NSSBΔ21-enriched fractions were selected with a Bradford colorimetric assay, and NSSBΔ21 purity was determined by SDS–PAGE analysis with Coomassie staining. Purified NSSBΔ21 fractions were pooled and dialyzed against a buffer containing 5 mM Tris (pH 7.5), 0.2 M sodium acetate, 1 mM DTT, 1 mM EDTA, and 10% glycerol. NSSBΔ21 purity was >98%.

HCV-NSSBΔ21 Polymerase Assay. An enzyme assay was used to measure inhibition of HCV-NSSBΔ21 polymerase activity. The cell-free HCV-NSSBΔ21 polymerase assay is based on the amount of double-stranded RNA synthesized in the presence of HCV-NSSBΔ21, a homopolymeric RNA template (Poly U, GE Healthcare, Chalfont St. Giles, U.K.) and ATP, measured with an intercalating agent (SYBR Green, Applied Biosystems), as previously described.³² The Quik-Change site-directed mutagenesis kit (Stratagene, La Jolla, CA) was

used to assess the effect of amino acid substitutions conferring resistance to other specific HCV RdRp inhibitors. The tested substitutions included M423T, C316Y, H95Q, and P495L. The constructs were verified by DNA sequencing, and the corresponding proteins were purified as described above. Each experiment was performed in triplicate.

Cytotoxicity Assay. Exponentially growing HuH7 and HEK293 cells were trypsinized and plated (2000 and 1000 cells per well, respectively) in 96-well microplates and allowed to attach for 96 h at 37 °C under 5% CO₂. A 200 μL aliquot of drug solution, diluted in medium with 1% DMSO (final concentration), was added and the cells were incubated for 72 h at 37 °C under 5% CO₂. The drug was evaluated at different concentrations ranging from 0 to 512 μM. Cytotoxicity was evaluated with a 3-(4,5-dimethylthiazol-2-yl)-2,5-diphenyltetrazolium bromide colorimetric assay (MTT assay). Each experiment was performed in triplicate.

■ ASSOCIATED CONTENT

S Supporting Information. Additional experimental details and ¹H NMR, ¹³C NMR, and MS data for all compounds. This material is available free of charge via the Internet at <http://pubs.acs.org>.

■ AUTHOR INFORMATION

Corresponding Author

*Phone: (33) 4 76 63 53 11. Fax: (33) 4 76 63 52 98. E-mail: Ahcene.Boumendjel@ujf-grenoble.fr.

Author Contributions

[†]These authors made equal contributions to this work.

Author Contributions

[∞]These authors are equal senior investigators in this study.

■ ACKNOWLEDGMENT

R.H. is a recipient of a fellowship grant from the Ministère de l'Enseignement et de la Recherche, for which he is very thankful. A part of the project related to this article is funded by l'Agence Nationale de la Recherche (ANR). W.Y. is a recipient of a fellowship from the University of Sun Yat-Sen (China), for which he is thankful.

■ ABBREVIATIONS USED

DMF, dimethylformamide; DMSO, dimethylsulfoxide; DTT, dithiothreitol; EDTA, ethylenediaminetetraacetic acid; HCV, hepatitis C virus; MMFF94, Merck molecular force field 94; MTT, 3-(4,5-dimethylthiazol-2-yl)-2,5-diphenyltetrazolium bromide; NSSB, nonstructural 5B protein; PDB, Protein Data Bank; peg-IFN, pegylated interferon; RBV, ribavirin; RdRp, RNA-dependent RNA polymerase; TFA, trifluoroacetic acid; Tris, tris(hydroxymethyl)aminomethane; WHO, World Health Organization; Wt, wild-type

■ REFERENCES

- (1) Wong, T.; Lee, S. S. Hepatitis C: a review for primary care physicians. *Can. Med. Assoc. J.* **2006**, *174*, 649–659.
- (2) Pawlotsky, J.-M.; McHutchison, J. G. Hepatitis C. Development of new drugs and clinical trials: promises and pitfalls. *Hepatology* **2004**, *39*, 554–567.

- (3) Strader, D. B.; Wright, T.; Thomas, D. L.; Seeff, L. B. Diagnosis, management, and treatment of hepatitis C. *Hepatology* **2004**, *39*, 1147–1171.
- (4) Dixit, N. M.; Layden-Almer, J. E.; Layden, T. J.; Perelson, A. S. Modelling how ribavirin improves interferon response rate in hepatitis C virus infection. *Nature* **2004**, *432*, 922–924.
- (5) Feld, J. J.; Hoofnagle, J. H. Mechanism of action of interferon and ribavirin treatment of hepatitis C. *Nature* **2005**, *436*, 967–972.
- (6) Zein, N. N. Clinical significance of hepatitis C virus genotypes. *Clin. Microbiol. Rev.* **2000**, *223*–225.
- (7) Carroll, S. S.; Olsen, D. B. Nucleoside analog inhibitors of hepatitis C virus replication. *Infect. Disord.: Drug Targets* **2006**, *6*, 17–29.
- (8) Beaulieu, P. L. Recent advances in the development of NSSB polymerase inhibitors for the treatment of hepatitis C virus infection. *Expert Opin. Ther. Pat.* **2009**, *19*, 145–164.
- (9) Pauwels, F.; Mostmans, W.; Quirynen, L. M. M.; van der Helm, L.; Boutton, C. W.; Rueff, A.-S.; Cleiren, E.; Raboisson, P.; Surlaux, D.; Nyanguile, O.; Simmen, K. A. Binding-site identification and genotype profiling of hepatitis C virus polymerase inhibitors. *J. Virol.* **2007**, *81*, 6909–6919.
- (10) Beaulieu, P. L.; Bös, M.; Bousquet, Y.; Fazal, G.; Gauthier, J.; Gillard, J.; Goulet, S.; LaPlante, S.; Poupert, M.-A.; Lebeuvre, S.; McKercher, G.; Pellerin, C.; Austel, V.; Kukolj, G. Non-nucleoside inhibitors of the hepatitis C virus NSSB polymerase: discovery and preliminary SAR of benzimidazole derivatives. *Bioorg. Med. Chem. Lett.* **2004**, *14*, 119–124.
- (11) Harper, S.; Pacini, B.; Avolio, S.; Di Filippo, M.; Migliaccio, G.; Laufer, R.; De Francesco, R.; Rowley, M.; Narjes, F. Development and preliminary optimization of indole-*N*-acetamide inhibitors of hepatitis C virus NSSB polymerase. *J. Med. Chem.* **2005**, *48*, 1314–1317.
- (12) Stansfield, I.; Ercolani, C.; Mackay, A.; Conte, I.; Pompei, M.; Koch, U.; Gennari, N.; Giuliano, C.; Rowley, M.; Narjes, F. Tetracyclic indole inhibitors of hepatitis C virus NSSB-polymerase. *Bioorg. Med. Chem. Lett.* **2009**, *19*, 627–632.
- (13) Habermann, J.; Capito, E.; del Rosario Rico Ferreira, M.; Koch, U.; Narjes, F. Discovery of pentacyclic compounds as potent inhibitors of hepatitis C virus NSSB RNA polymerase. *Bioorg. Med. Chem. Lett.* **2009**, *19*, 633–638.
- (14) Goulet, S.; Poupert, M.-A.; Gillard, J.; Poirier, M.; Kukolj, G.; Beaulieu, P. L. Discovery of benzimidazole-diamide finger loop (thumb pocket I) allosteric inhibitors of HCV NSSB polymerase: implementing parallel synthesis for rapid linker optimization. *Bioorg. Med. Chem. Lett.* **2010**, *20*, 196–200.
- (15) Beaulieu, P. L.; Jolicoeur, E.; Gillard, J.; Brochu, C.; Coulombe, R.; Dansereau, N.; Duan, J.; Garneau, M.; Jakalian, A.; Kühn, P.; Lagacé, L.; LaPlante, S.; McKercher, G.; Perrault, S.; Poirier, M.; Poupert, M.-A.; Stammers, T.; Thauvette, L.; Thavonekham, B.; Kukolj, G. *N*-Acetamidoleucinecarboxylic acid allosteric “finger-loop” inhibitors of the hepatitis C virus NSSB polymerase: discovery and initial optimization studies. *Bioorg. Med. Chem. Lett.* **2010**, *20*, 857–861.
- (16) Beaulieu, P. L.; Dansereau, N.; Duan, J.; Garneau, M.; Gillard, J.; McKercher, G.; LaPlante, S.; Lagacé, L.; Thauvette, L.; Kukolj, G. Benzimidazole thumb pocket I finger-loop inhibitors of HCV NSSB polymerase: improved drug-like properties through C-2 SAR in three sub-series. *Bioorg. Med. Chem. Lett.* **2010**, *20*, 1825–1829.
- (17) Narjes, F.; Crescenzi, B.; Ferrara, M.; Habermann, J.; Colarusso, S.; del Rosario Rico Ferreira, M.; Stansfield, I.; Mackay, A. C.; Conte, I.; Ercolani, C.; Zaramella, S.; Palumbi, M.-C.; Meuleman, P.; Leroux-Roels, G.; Giuliano, C.; Fiore, F.; Di Marco, S.; Baiocco, P.; Koch, U.; Migliaccio, G.; Altamura, S.; Laufer, R.; De Francesco, R.; Rowley, M. Discovery of (7*R*)-14-cyclohexyl-7- $\{[2-(dimethylamino)ethyl](methylamino)-7,8-dihydro-6*H*-indolo[1,2-*e*][1,5]benzoxazocine-11-carboxylic acid (MK-3281), a potent and orally bioavailable finger-loop inhibitor of the hepatitis C virus NSSB polymerase. *J. Med. Chem.* **2011**, *54*, 289–301.$
- (18) Study To Evaluate the Safety, Tolerability and Pharmacokinetics of MK-3281 in Healthy and Hepatitis C Infected Male Patients; Trial NCT00635804; National Institutes of Health, Bethesda, MD, U.S., 2008; <http://clinicaltrials.gov/ct2/show/NCT00635804>.
- (19) Boumendjel, A. Aurones: a subclass of flavones with promising biological potential. *Curr. Med. Chem.* **2003**, *10*, 2621–2630.
- (20) Seikel, M. K.; Geissman, T. A. Anthochlor pigments. VII. The pigments of yellow *Antirrhinum majus*. *J. Am. Chem. Soc.* **1950**, *72*, 5725–5730.
- (21) Nakayama, T.; Yonekura-Sakakibara, K.; Sato, T.; Kikuchi, S.; Fukui, Y.; Fukuchi-Mizutani, M.; Ueda, T.; Nakao, M.; Tanaka, Y. Aureusidin synthase: a polyphenol oxidase homolog responsible for flower coloration. *Science* **2000**, *290*, 1163–1166.
- (22) Varma, S.; Varma, M. Alumina-mediated condensation. A simple synthesis of aurones. *Tetrahedron Lett.* **1992**, *33*, 5937–5940.
- (23) Beney, C.; Mariotte, A.-M.; Boumendjel, A. An efficient synthesis of 4,6-dimethoxy aurones. *Heterocycles* **2001**, *55*, 967–972.
- (24) Büchi, G.; Weinreb, M. Total syntheses of aflatoxins M₁ and G₁ and an improved synthesis of aflatoxin B₁. *J. Am. Chem. Soc.* **1971**, *93*, 746–752.
- (25) Okombi, S.; Rival, D.; Bonnet, S.; Mariotte, A.-M.; Perrier, E.; Boumendjel, A. Discovery of benzylidenbenzofuran-3(2*H*)-one (aurones) as inhibitors of tyrosinase derived from human melanocytes. *J. Med. Chem.* **2006**, *49*, 329–333.
- (26) Brehm, C.; Zimmermann, P. J.; Zemolka, S.; Palmer, A.; Buhr, W.; Postius, S.; Simon, W.-A.; Herrmann, M. Pharmaceutically Active Dihydrobenzofurane-Substituted Benzimidazole Derivatives. Patent WO 2008/084067, July 17, 2008.
- (27) Kodra, J. T.; Madsen, P.; Lau, J.; Jorgensen, A. S.; Christensen, I. T. Novel Glucagon Antagonists. Patent WO 2003/048109, June 12, 2003.
- (28) Ahmed-Belkacem, A.; Ahnou, N.; Barbotte, L.; Wychowski, C.; Pallier, C.; Brillet, R.; Pohl, R.-T.; Pawlotsky, J.-M. Silibinin and related compounds are direct inhibitors of hepatitis C virus RNA-dependant RNA polymerase. *Gastroenterology* **2010**, *138*, 1112–1122.
- (29) Kwong, A. D.; McNair, L.; Jacobson, I.; George, S. Recent progress in the development of selected hepatitis C virus NS3-4A protease and NSSB polymerase inhibitors. *Curr. Opin. Pharmacol.* **2008**, *8*, 522–531.
- (30) Hashimoto, H.; Mizutani, K.; Yoshida, A. Fused Cyclic Compounds and Medicinal Use Thereof. Patent WO 2003/000254, January 3, 2003.
- (31) Ikegashira, K.; Oka, T.; Hirashima, S.; Noji, S.; Yamanaka, H.; Hara, Y.; Adachi, T.; Tsuruha, J.-I.; Doi, S.; Hase, Y.; Noguchi, T.; Ando, I.; Ogura, N.; Ikeda, S.; Hashimoto, H. Discovery of conformationally constrained tetracyclic compounds as potent hepatitis C virus NSSB RNA polymerase inhibitors. *J. Med. Chem.* **2006**, *49*, 6950–6953.
- (32) Wakita, T.; Pietschmann, T.; Kato, T.; Date, T.; Miyamoto, M.; Zhao, Z.; Murthy, K.; Habermann, A.; Krausslich, H. G.; Mizokami, M.; Bartenschlager, R.; Liang, T. J. Production of infectious hepatitis C virus in tissue culture from a cloned viral genome. *Nat. Med.* **2005**, *11*, 791–796.